

# Classifying Numerical Geometric, Color and Texture Features of Normal and Abnormal Red Blood Cells Features using Support Vector Machine

<sup>[1]</sup> Jameela Ali Alkrimi\*, <sup>[2]</sup> Loay E. George, <sup>[3]</sup> Rafah M. Almuttairi, <sup>[4]</sup> Zainab Abood Ahmed AL -Bairmani, <sup>[5]</sup> Safaa Hakeem al-Khafaji, <sup>[6]</sup> Ameer Hamdi Hakeem Al-Ameedee

<sup>[1]</sup> <sup>[5]</sup> <sup>[6]</sup> College of Dentistry, University of Babylon, Babylon, Iraq

<sup>[2]</sup> University of Information Technology & Communication, Baghdad, Iraq

<sup>[3]</sup> College of Information Technology Engineering, Al-Zahraa University for Women, Karbala, Iraq

<sup>[4]</sup> Department of Studies and Planning, University of Babylon, Babylon, Iraq

Emails ID: <sup>[1]</sup> dent.jameela.ali@uobaby.on.edu.iq, <sup>[2]</sup> loayedwar57@scbaghdad.edu.iq, <sup>[4]</sup> zanab.abboud@uobabylon.edu.iq, <sup>[5]</sup> Safaahaem74@gmail.com, <sup>[6]</sup> ameeralameedee@gmail.com

**Abstract**— This paper focuses on extracting the geometric, texture, and color numerically of red blood cells (RBCs). Several image processing processes were to segment and isolate 1000 individual RBC from the Cytoplasm. The isolation individual of blood cells was classified using three sets of integrated features. The first set, which only included geometrical features, was used to determine whether the tested blood cells were non-spherical or had a spherical shape. The types of spherical and non-spherical cells were identified using the second set, which mostly consisted of textural characteristics. The third set, consisting the color of cells. Support vector machines (SVMs) as classification algorithm was apply to tested the features. It achieves 98% classification accuracy. The performance of a classification algorithm gives a Precision 98%, recall 97%, and Kappa statistic 0.968.

**Index Terms**— *Image processing. Features extraction. Red blood cells. Support vector machines. Evaluation.*

## I. INTRODUCTION

Technology in the medical industry is currently developing in step with the times. The use of technology has grown essential in all fields, particularly the biomedical one. Numerous methods have been created to assist medical professionals in diagnosing a certain illness. Digital image processing can be used for lung, liver, and bone problems, as well as for the detection of uterine tumors and cancer. It can also be used for microscopic image analysis (Singh, 2023) (Jiang, 2023) (Rahmat, 2018).

Medical images aid in the diagnosis of numerous blood illnesses as well as the identification and treatment of these conditions (Anwar, 2018). Many different types of medical images have been analyzed using this technique to extract more pertinent medical data from the images to aid in clinical diagnosis. Physicians can be helped to improve treatment regimens and forecast outcomes of treatment by utilizing an efficient and automatic cell classification method (Shen, 2017) (Cai, 2022) (Song, 2021).

An essential task in the medical industry is the analysis of the patient's blood sample. Numerous health problems can be attributed to abnormalities in blood cells. One of the main components of blood is red blood cells, or RBCs. We can diagnose several disorders by using the RBC classification system (Parab, 2021) (Foy et al, 2023).

RBCs in blood can be either normal or abnormal; abnormal RBCs differ in their forms, colors, and sizes. By looking at the external edge and core pallor area of RBCs in photos, one

may tell if they are normal or abnormal (Alkrimi, 2019) (Dhar, 2023). Anemia is the most prevalent condition that these traits can indicate, but they can also indicate other blood problems linked to red blood cells, such as kidney tumours, anemia, malnutrition, and hemolytic disease. Due to changes in the morphology of the RBC. The variation morphology of RBCs produces a huge number of features for normal or abnormal RBCs (Tyrrell, 2021) (Strohm, 2013). Any divergence in size, shape, volume, structure, or colour indicates an aberrant cell. Generally speaking, normal red blood cells have a pale centre and are biconcave in shape. Genetic or acquired pathological disorders can have a significant impact on this RBC characteristic (Adewoyin et al., 2019; Klik et al., 2023). Four characteristics of red blood cell shape need to be assessed: hue, dimensions, form, and inclusions (Barger, 2022) (Alkrimi, 2021).

Pre-processing, image segmentation, feature extraction, and image detection are the main processes in image analysis. To enable us to identify the precise properties of the blood cells, image segmentation, and feature extraction are the most crucial and difficult steps. The goal of extracting features from images is to retrieve objects of interest (Dhal, 2023). A lot of research works have been done on the extracted RBCs features. Mahmood et al. used geometric features and the Hough transform to determine the center of RBCs (Patel, 2023) (Alferez et al, 2019) (Alkrimi, 2019). Maji et al. indicated that RBCs could have been automatically classified using mathematical morphology (Ajagbe, 2023) (Mahmood, 2012). Rahman et al. identified an anomaly in red blood cells, white blood cells, and platelets in an anemic state using

a neural network. Ali et al. analysis and extraction geometric and shape of features of red blood cells (Rahman et al., 2012) (Wong, 2021).

Blood cell classification research involves a variety of features. To achieve an accurate classification, features must be chosen carefully. Certain characteristics, such as geometry, color, texture, and shape, are frequently used (Ajagbe, et al. 2023) (Bianconi, 2021) (Ali, 2013) (Alzubaidi, 2020) (Song W. H., 2021).

## II. METHODOLOGY

The method suggested for automatic extraction system of the blood cell is shown in Figure 1. In this work, 1000 colour microscopy pictures of RBCs were categorised as normal or aberrant. The pictures were taken from our collection. The pictures were taken from 200 haematology slides that displayed various blood diseases. The medical personnel of SEGI University in Malaysia has confirmed the medical aspects of all the photos.

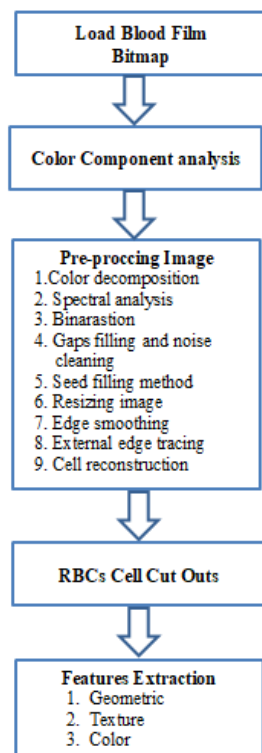


**Figure 1.** Automatic feature extraction system

### A. Image Acquisition

The original blood film of a patient from the haematology department at Serdang Hospital in Selangor, Kuala Lumpur, Malaysia, provided the images from which the dataset was compiled. Blood film was transferred to pictures in 2013 using an Olympus BX43 photo imaging microscope (Olympus, Japan) fitted with a U-CAM 3D camera. The images show in figure 2.

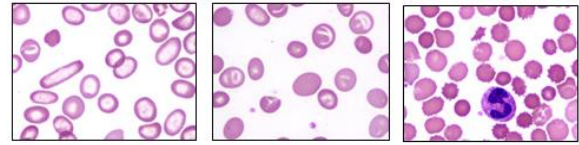


**Figure 2.** blood smear images

### B. Pre-processing Image

According to the first step, every image processing operation must identify the colours of the backdrop and the target and isolate the target's cell area from its surroundings. Next, the cell cut-out's internal and external borders of the central pallor area pixels were drawn. The adopted geometrical properties, which have been employed to characterise the forms of RBCs, were then ascertained using the trace points: Fourier descriptors, aspect ratio, and moments. In order to assess the spatial colour variation inside the RBC, additional textural features were computed.

Pre-processing involves a number of image processing operations which are performed in ten complementary steps. These steps include analyzing the color contents of the input cell image to separate target colors from background colors, performing image binarization to separate target pixels from background pixels, and then segmenting cells using the boundary tracing method. The color heterogeneity of the background and cell pixels, that was a major issue we encountered in this work, is caused by the employment of several paints to improve the blood test samples' visual appearance, shown in Figure 3.

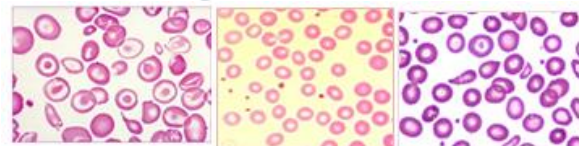


**Figure 3.** color variable blood smear images

In order to complete this challenge, we spread the colour of each pixel around two dominants. To complete this challenge, we spread the colour of each pixel around two dominants. To achieve the obtain the optimal segmentation process, several procedures are useful. The following could be used to summarize the steps that were implemented in the pre-processing our system;

#### Step 1:

Scan the pixels inside the strip that encircles the image border area (of width= $w$ ; for example, let's assume  $w=5$ ). The initial centroid of the background colour will be created using the average values of the colour components of the pixels inside the strip since it is assumed that the majority of the pixels inside this surrounding area are background pixels.

#### Step 2:

Similarly, the center points of the target (cells) pixels are initially established by scanning the pixels in the interior region of the images and calculating the average values of their colors.

**Step 3:**

Use the following equations to increase the distance between the target centroids and the starting background:

Where;

The red, green, and blue background's central components are denoted by (Rb,Gb,Bb).  $\alpha$  is the parameter for separation.

**Step 4:**

Assign each and every image pixel to one of the two clusters (background or cell) based on how far off they are from the respective centroids (background or cell).

**Step 5:**

Using the following formulas, find the average color components for every pixel indexed as background:

where b: is the set of image pixels indexed as background. nb: is the size of the set (b).

**Step 6:**

Use the following formulas to find the average color components for every pixel identified as target (or cell):

Were

The collection of pixels indexed as cell pixels is denoted by c. nc: represents the set's length (or size) (c).

**Step 7:**

Utilising the following distance measure, compare the difference (D) between the vectors and (Rb,Gb,Bb) and between the vectors and (Rc,Gc,Bc):

**Step 8:**

Normal RBC RBCs for different diseases

Repeat steps 4 through 7 if D is greater than the predetermined threshold value (Dmin); if not, exit the system. The optimal segmentation process results show in figure 4.

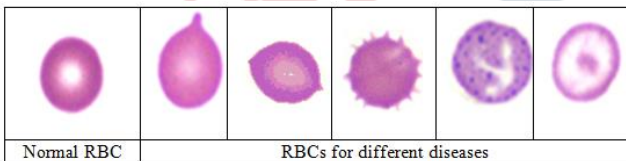


**Figure 4.** individual RBCs image

**III. FEATURE EXTRACTION OF RBCS**

Feature extraction is one of the important stages of the classification of the RBC image. The shape, color, and texture are the most important features of the RBC cell image are based on the characteristics of RBCs on the Hematology category's classification blood cells (Alkrimi et al., 2014) (Aliyu, 2019). This paper Applying statistical features as; extract shape RBCs features the include size, Fourier Descriptor and Packing, Where the method applied for extracting of the texture and color feature was Gray-Level, Contracts and moment.

The objectives of this research is to extracted numerical geometric color and texture features for normal and abnormal RBCs and create a data set of RBCs. The geometric features

are based on the external and internal boundary (central pallor) RBC. A powerful feature analysis technique through calculating the most important features; cell size, shape, parameter length, irregularity shape measure and elongation shape measure.

In order to make feature extraction process easier, 1000 RBCs images was grouped into 8 groups; normal and 7 abnormal bases on the dominant feature of the external shape, the pallor central area, color and whether contains body or not as munition (Alkrimi, 2019). Figure 5 show the RBCs group. Each group have different number sample of RBCs ranged (80-150).

Normal ab normal RBCs type

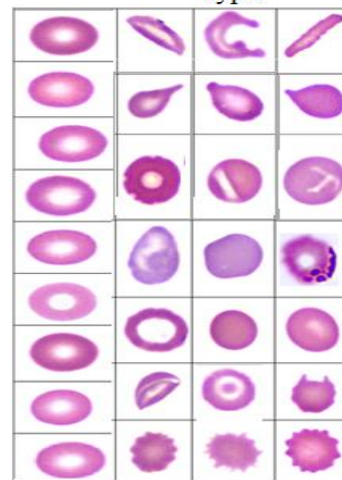


**Figure 5.** groups of RBCs

The statistical features as variance, contrast, moment of RBCs can be described by a set of texture features. As mentioned in [16], this set of features holds the following sub-sets of features;

- The colour component histogram moments (up to the fifth order) and the associated grayscale image.
- The colour component and grey value spatial moments (the centre of mass is used as the pivot point).
- The moments in the contrast histogram for each colour and grey component.
- Each grey component's gradient histogram moments.
- The collection of external border Fourier descriptors.
- An extracted cell's aspect ratio (f).
- The centre pallor boundary's relative size within the cell.
- Additional shading homogeneity measurements.
- The n in the features that presented the number of applications, in sun of the  $n = 2$  that mean (X, Y) where  $n=4$  it means (red, blue, green and gray)

**A. Aspect ratio**

A popular way to define a form is to compare its width to its height, which is expressed as the aspect ratio.



**B. Packing features;**

$$Packing = \frac{(No\ of\ External\ Boundary\ Pixels)^2}{Total\ No\ of\ Cell\ Pixels}$$

**C. Fourier Descriptor**

$$F_a(n) = \frac{T}{2\pi^2 n^2} \sum_{i=1}^M \frac{\Delta x(i)}{\Delta t(i)} [\cos(\frac{2\pi}{T} \sum_{j=1}^i \Delta t(j)) - \cos(\frac{2\pi}{T} \sum_{j=1}^{i-1} \Delta t(j))]$$

Where,

$\{x_0, x_1, x_2, \dots, x_M\}$  are the x-coordinates of external boundary points.

$\{y_0, y_1, y_2, \dots, y_M\}$  are the y-coordinates of external boundary points.

M is the number of boundary points.

$$\Delta x(i) = x(i) - x(i-1)$$

$$\Delta y(i) = y(i) - y(i-1)$$

$$\Delta t(i) = \sqrt{(\Delta x(i))^2 + (\Delta y(i))^2}$$

$$T = \sum_{i=1}^M \Delta t(i)$$

**D. Absolute Moment**

$$aMon(n) = \frac{1}{k} \left| \sum_{i \in c} (x'_i + jy'_i)^n \right|, \quad n = 1, 2, 3, 4$$

Where,

$$x'_i = \frac{1}{L} [(x_i - \bar{x}) \cos \theta - (y_i - \bar{y}) \sin \theta]$$

$$y'_i = \frac{1}{L} [(x_i - \bar{x}) \sin \theta + (y_i - \bar{y}) \cos \theta]$$

**E. Variance**

$$\sigma^2 = \frac{\sum_{i=1}^n (x_i - \bar{x})^2}{N}$$

Where;

$x_i$  = Each value in the data set

$\bar{x}$  = Mean of all values in the data set

N = Number of values in the data set

**F. Contracts**

$$aCnt(n) = \frac{aVr(n)}{\bar{X}}, \quad n = 1, 2$$

**IV. THE RESULTS**

This section details the results from all statistical features that amination in section 3 above. The average of each group shows in Table 1. The features were tested with the SVM clarification algorithm using WEKA software. The classification achieves high accuracy about 97.8%. The result of classifier visualizes for the 8 RBCs type data set shown in Figure6.

**Table I. RBCs Features**

RBCs		Features of RBCs					
Type	Image	Size (pixel)	Aspect ratio	Fourier Descriptor	Variance	Contracts	Moment
Normal		28610.8	10.69569	0.422511	0.926877	124.1738	1.436944
Ablong		35147.76	15.38508	0.47325	0.694268	113.433	1.096733
Piko		34177.11	14.45012	0.461162	0.669687	113.2114	0.975188
Include body		31575.85	13.60711	0.405079	0.856351	96.26693	1.076095
With shadow		32793.11	13.09656	0.437551	0.860296	106.4151	1.116178
Rounded		30694.27	10.94298	0.367175	0.934688	120.2667	1.414135
Schist		30664.47	14.94442	0.482197	0.751295	114.3004	1.087966
Spuki		28449.28	13.83406	0.393144	0.845506	128.514	1.386399

**Table II: The result classification algorithms**

Accuracy	Precision	Sensitivity	Specificity	Kappa Statistic	F-scor
97.8%	98	98.4	86.8	0.968	0.99

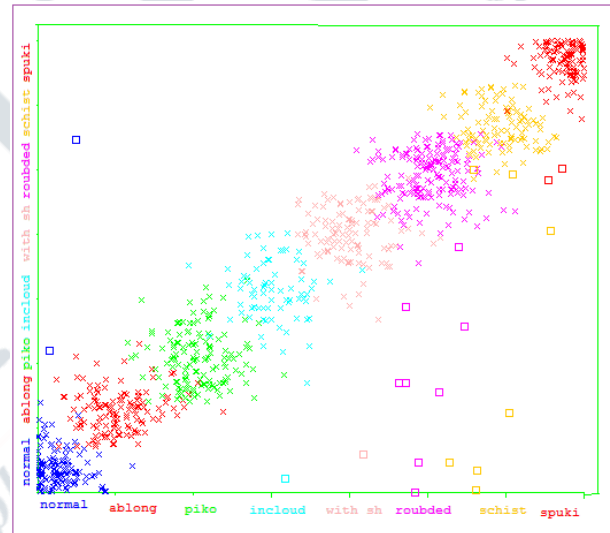


**Figure 6.** Classifier visualizes the result of 8 RBCs type data set

**V. CONCLUSION**

This work mainly aimed to extracted features of normal and abnormal RBCs. The features extracted are geometric, texture and color numerically. Several image processing process in order to segmented and isolation 1000 individual RBC from Cytoplasm. These RBCs created an balance data set. The statistic features are such as size, Fourier Descriptor and Packing extracted for shape, where the Variance, Contracts and Moment for extract the texture and color image. Support vector machines (SVMs) as classification algorithm was apply to tested the features. It achieve 97.8% classification accuracy. The performance of a classification algorithm give precision98%, sensitivity98.4%, specificity86.8%, Kappa statistic 0.968 and F-scor 0.99

**REFERENCES**

- [1] Adewoyin, A. S. (2019). Erythrocyte morphology and its disorders. *Erythrocyte*, pp. 1-10.
- [2] Ajagbe, S. A.-A. (2023). Investigating Two-Stage Detection Methods Using Traffic Light Detection Dataset. In *Object Tracking Technology: Trends, Challenges and Applications*. Singapore: Springer Nature Singapore., pp. pp. 249-274.
- [3] Alférez, S. M. (2019). Color clustering segmentation framework for image analysis of malignant lymphoid cells in peripheral blood. *Medical & biological engineering & computing*, pp. 57, .1265-1283.
- [4] Ali, J. A. (2013). Red blood cell recognition using geometrical features. *International Journal of Computer Science Issues (IJCSI)*, pp. 10(1), 90.
- [5] Aliyu, H. A. (2019, 14(1),). *Indonesian Journal of Electrical Engineering and Computer Science.*, pp. 100-104.
- [6] Alkrimi, J. A. (2019). New normal and abnormal red blood cells features for improved classification. *International Journal of Computer*, pp. 32(1), 1-8.
- [7] Alkrimi, J. A., George, L. E., Suliman, A., Ahmad, A. R., & Al-Jashamy, K. (2014). Isolation and classification of red blood cells in anemic microscopic images. *World Academy of Science, Engineering and Technology, International Journal of Medical, Health, Biomedical, Bioengineering and Pharmaceutical Engineering*, 8, 727-730.
- [8] Alkrimi, Jameela Ali, Rajaa Salih Mohammed Hasin, Ali Zaki Naji, Loay E. George, and Sherna Aziz Tome. "Classification of Imbalanced leukocytes Dataset using ANN-based Deep Learning." In *Journal of Physics: Conference Series*, vol. 1999, no. 1, p. 012140. IOP Publishing, 2021.
- [9] Alzubaidi, L. F.-S. (2020). Deep learning models for classification of red blood cells in microscopy images to aid in sickle cell anemia diagnosis. *Electronics*, pp. 9(3), 427.
- [10] Anwar, S. M. (2018). Medical image analysis using convolutional neural networks: a review. *Journal of medical systems*, pp. 42, 1-13.
- [11] Bacus J, W. J. (1977). An automated method of differential red blood cell classification with application to the diagnosis of anemia. *Journal of Histochemistry & Cytochemistry.*, pp. ;25(7):614-32.
- [12] Barger, A. M. (2022). Erythrocyte morphology. *Schalm's veterinary hematology*, pp. 188-197.
- [13] Bianconi, F. F. (2021). Colour and texture descriptors for visual recognition: A historical overview. *Journal of Imaging*, pp. 7(11), 245.
- [14] Cai, L. G. (2022). A review of the application of deep learning in medical image classification and segmentation. *Annals of translational medicine*, p. 8(11).
- [15] Dhal, K. G. (2023). Illumination-Free Clustering Using Improved Slime Mould Algorithm for Acute Lymphoblastic Leukemia Image Segmentation. *Journal of Bionic Engineering*, pp. 1-19.
- [16] Dhar, P. K. (2023). HPKNN: Hyper-parameter optimized KNN classifier for classification of poikilocytosis. *International Journal of Imaging Systems and Technology*, pp. 33(3), 928-950.
- [17] Foy, B. H.-S. (2023). Computer vision quantitation of erythrocyte shape abnormalities provides diagnostic, prognostic, and mechanistic insight. *Blood Advances*, pp. 7(16), 4621-4630.
- [18] Jiang, M. S. (2022). Automatic classification of red blood cell morphology based on quantitative phase imaging. *International Journal of Optics*.
- [19] Jiang, X. H. (2023). Deep learning for medical image-based cancer diagnosis. *Cancers*, pp. 15(14), 3608.
- [20] Klbik, I. (2023, 04.). On the involvement of cell volume regulation mechanisms in post-hypertonic lysis and slow-freezing injury of human erythrocytes and its broader cryobiological significance. *bioRxiv*, -.
- [21] Mahmood, N. H. (2012). Red blood cells estimation using Hough transform technique. *Signal & Image Processing*, pp. 3(2), 53.
- [22] Parab, M. A. (2021). Red blood cell classification using image processing and CNN. *SN Computer Science*, pp. 2(2), 70.
- [23] Patel, A. V. (2023). Single-Object Detection from Video Streaming. In *Object Tracking Technology: Trends, Challenges and Applications*. Singapore: Springer Nature Singapore, pp. pp. 1-21.
- [24] Rahman, S. A. (2012). Automatic identification of abnormal blood smear images using color and morphology variation of RBCS and central pallor. *Computerized Medical Imaging and Graphics*, pp. 87, 101813.
- [25] Rahmat, R. F. (2018, February). The morphological classification of normal and abnormal red blood cell using self organizing map. In *IOP Conference Series: Materials Science and Engineering (Vol.*

- [26] Shen, D. W. (2017). Deep learning in medical image analysis. Annual review of biomedical engineering, pp. 19, 221-248.
- [27] Singh, S. S. (2023). Industry 4.0 Internet of Medical Things Enabled Cost Effective Secure Smart Patient Care Medicine Pouch. In: Nayyar, A., Naved, M., Rameshwar, R. (eds). In New Horizons for Industry 4.0 in Modern Business. Cham: Springer International, pp. pp. 149-170.
- [28] Song, W. H. (2021). Red blood cell classification based on attention residual feature pyramid network. Frontiers in Medicine, pp. 8, 741407.
- [29] Song, W. H. (2021). Red blood cell classification based on attention residual feature pyramid network. Frontiers in Medicine, pp. 8, 741407.
- [30] Strohm, E. M. (2013). Probing red blood cell morphology using high-frequency photoacoustics. Biophysical journal, pp. 105(1), 59-67.
- [31] Tyrrell, L. R. (2021). Morphologic changes in red blood cells: An illustrated review of clinically important light microscopic findings. The Malaysian Journal of Pathology, pp. 43(2), 219-239.
- [32] Wong, A. A. (2021). Analysis of vision-based abnormal red blood cell classification. arXiv preprint arXiv, p. 2106.00389.

